COLOUR DIPOLE PHENOMENOLOGY

G. SHAW*

Particle Physics Group,
School of Physics and Astronomy,
The University of Manchester,
Manchester M13 9PL, U.K.
E-mail: graham.shaw@manchester.ac.uk

Recent, precise HERA data on diffractive photoprocesses are analysed in the context of colour dipole models. The data on the deep inelastic structure function F_2 is used to determine the dipole cross section, and shown to prefer parameterisations which include saturation effects. The resulting dipole cross sections are then used to predict cross sections for DVCS and DDIS, which are in good agreement with experiment.

1. The colour dipole model

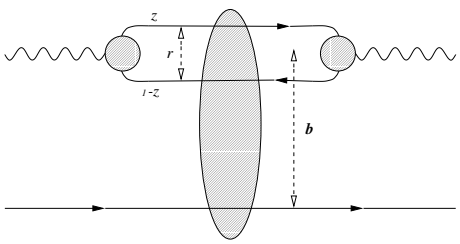

Figure 1. The colour dipole model for elastic Compton scattering $\gamma^* p \to \gamma^* p$ and Deeply Virtual Compton Scattering (DVCS) on protons, $\gamma^* p \to \gamma p$

In the colour dipole model [1,2], the forward amplitude for virtual Compton scattering is assumed to be dominated by the mechanism illustrated in Figure 1 in which the photon fluctuates into a $q\bar{q}$ pair of fixed transverse

*This work describes work carried out in collaboration with J. R. Forshaw.

separation r and the quark carries a fraction z of of the incoming photon light-cone energy. Using the optical theorem, this leads to

$$\sigma_{\gamma^* p}^{L,T} = \int dz\, d^2r\, |\psi_{L,T}(z,r,Q^2)|^2 \sigma(s^*,r) \tag{1}$$

for the total virtual photon-proton cross section, where $\psi_{L,T}(z,r,Q^2)$ are the appropriate spin-averaged light-cone wavefunctions of the photon and $\sigma(s^*,r)$ is the dipole cross section. As implied, the dipole cross section is usually assumed to be independent of z (see below), and is parameterized in terms of an energy variable s^* which depends on the model.

For small r, the light-cone photon wavefunctions are given by tree level QED expressions [1,3], which decay exponentially at large r, with typical r-values of order Q^{-1} at large Q^2 and of order m_f^{-1} at $Q^2 = 0$. However for large dipoles $r \geq 1$ fm, which are important at low $Q^2 \leq 4m_f^2$, a perturbative treatment is not really appropriate. Nonetheless, we still use the perturbative QED wavefunction, treating the quark mass as a parameter which can be used to adjust the wavefunction at large r-values. At high Q^2 where small dipoles dominate, the wavefunctions are insensitive to the quark mass.

The dipole cross section itself is described by models devised to incorporate various theoretical requirements, like colour transparency for small dipoles and soft hadronic behaviour for large dipoles. The parameters of the models are then determined by fitting to DIS structure function data, and the resulting dipole cross sections used to make predictions for other reactions, like DVCS (Deeply Virtual Compton Scattering) and especially DDIS (Diffractive Deep Inelastic Scattering), in order to test the model. Here we shall consider three such models. Since the details have been published elsewhere, we shall summarize their properties rather briefly.

The FS2004 Regge model This simple model[4] combines colour transparency for small dipoles $r < r_0$ with "soft pomeron" behaviour for large dipole sizes $r > r_1$ by assuming:

$$\begin{aligned} \sigma(x_m, r) &= A_H r^2 x_m^{-\lambda_H} \quad \text{for} \quad r < r_0 \quad \text{and} \\ &= A_S x_m^{-\lambda_S} \quad \text{for} \quad r > r_1, \end{aligned} \tag{2}$$

where

$$x_m = \frac{Q^2}{Q^2 + W^2} \left(1 + \frac{4m^2}{Q^2}\right). \tag{3}$$

For light quark dipoles, the quark mass m is a parameter in the fit, whilst for charm quark dipoles the mass is fixed at 1.4 GeV. In the intermediate region $r_0 \leq r \leq r_1$ we interpolate linearly between the two forms of (2).

If the boundary parameters r_0 and r_1 are kept constant then this parameterisation reduces to a sum of two powers, as might be predicted in a two pomeron approach, and can be thought of as an update of the original FKS Regge model [5] to accommodate the latest data (see below). It is plainly unsaturated, in that the dipole cross section obtained at small r-values and fixed Q^2 grows rapidly with increasing s (or equivalently with decreasing x) without damping of any kind.

The FS2004 Saturation model Saturation can be introduced into the above model by adopting a device previously utilized in [7]. Instead of taking r_0 to be fixed we now determine it to be the value at which the hard component is some fixed fraction of the soft component, i.e.

$$\sigma(x_m, r_0)/\sigma(x_m, r_1) = f \tag{4}$$

and treat f instead of r_0 as a fitting parameter. This introduces no new parameters compared to the Regge model. However, the scale r_0 now moves to lower values as x decreases, and the rapid growth of the dipole cross section at a fixed, small value of r begins to be damped as soon as r_0 becomes smaller than r. In this sense we model saturation, albeit crudely, with r_0 a saturation radius.

The CGC saturation model The above two models are closely related, allowing the introduction of saturation effects to be studied in a direct manner. In addition we shall consider the CGC dipole model of Iancu, Itakura and Munier [8], which purports to include the main features of the "Colour Glass Condensate" regime, and can be thought of as a more sophisticated version of the original "Saturation Model" of Golec-Biernat and Wüsthoff [9].

2. Analysis of the F_2 data

In this section, we shall fit the recent ZEUS data [10] in the kinematic range

$$0.045\,\mathrm{GeV}^2 < Q^2 < 45\,\mathrm{GeV}^2 \qquad x \leq 0.01\,. \tag{5}$$

This is identical to that used by Iancu et al. [8] to determine the parameters of the CGC saturation model, albeit neglecting charm. The corresponding

H1 data [11] can also be fitted, but it is necessary to float the relative normalization of the two data sets to achieve this, and we will not consider it here.

The best fit obtained with the FS2004 Regge model is shown as the dashed line in Figure 2. As can be seen, the quality of the fit is not good, corresponding to a χ^2/data point of 428/156. This is not just a failing of this particular parameterisation. We have attempted to fit the data with many other Regge inspired models, including the original FKS parameterizations [5,6], without success.

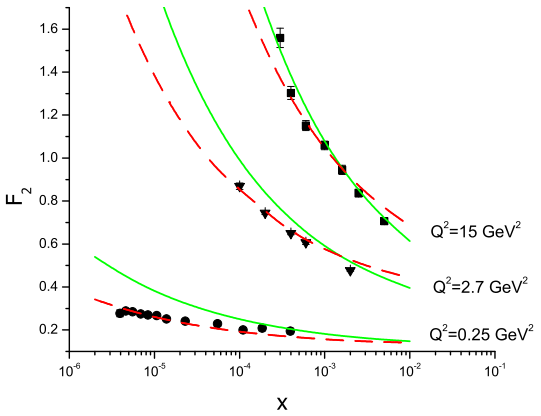

Figure 2. Comparison of the FS2004 Regge dipole fit (dashed line) to a subset of DIS data Also shown (solid line) is a fit of the same model to data in the restricted range $5 \times 10^{-4} < x < 10^{-2}$, extrapolated over the whole x-range $x < 0.01$.

A possible reason for this failing is suggested by the solid curve in Figure 2, which shows the result of fitting only to data in the x-range $5 \times 10^{-4} < x < 10^{-2}$, and then extrapolating the fit to lower x values, corresponding to higher energies at fixed Q^2. As can be seen, this leads to a much steeper dependence at these lower x-values (i.e. at higher energies) than is allowed by the data at all Q^2. An obvious way to solve this problem is by introducing saturation at high energies, to dampen this rise. This is confirmed by fitting with the FS2004 saturation model, which yields a χ^2/data point of 155/156. The resulting fit is shown in Figure 3, which also shows the very similar results previously obtained using the

more sophisticated CGC model (no charm fit) [8].

It is clear from these results that the introduction of saturation into the model immediately removes the tension between the soft and hard components which is so disfavoured by the data. However, it is important to note that this conclusion relies on the inclusion of the data in the low Q^2 region: both the Regge and saturation models yield satisfactory fits if we restrict to $Q^2 \geq 2\,\mathrm{GeV}^2$, with χ^2/data point values of 78/86 and 68/86 respectively.

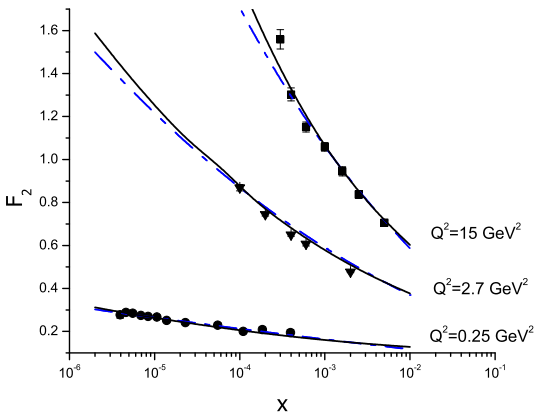

Figure 3. Comparison of the FS2004 saturation fit (solid line) to a subset of DIS data. Also shown (dot-dashed line) is the corresponding fit obtained using the CGC dipole model.

.

3. Predictions for other processes

One result of the above is that we now have well-determined parameterisations of the colour dipole cross section which, in the case of the FS2004, but not the CGC model, take account of charm. These can be used to yield predictions for other processes, in order to test the model against experimental data. Here we will compare these predictions with new, precise data on deeply virtual Compton scattering (DVCS) and, especially, diffractive deep inelastic scattering (DDIS). In doing so we stress that the photon wavefunctions and dipole cross sections used are precisely those determined in the previous section, without any adjustment of parameters. Predictions

can also be obtained for vector meson production processes, but these will not be considered here because of the large uncertainties associated with the badly known vector meson wavefunctions.

3.1. *Deeply virtual Compton scattering (DVCS)*

In the colour dipole model, the imaginary part of the scattering amplitude for deeply virtual Compton scattering

$$\gamma^* + p \to \gamma + p \,, \tag{6}$$

at zero momentum transfer is given by

$$\text{Im } A_{\text{DVCS}}(W^2, Q^2, t = 0) = \int dz \; \mathrm{d}^2 r \; \Psi_\gamma^{T*}(r, z, Q^2)\, \sigma(s, r)\, \Psi_\gamma^T(r, z, 0) \tag{7}$$

corresponding again to Figure 1. Thus dipole models provide predictions for the imaginary part of the forward amplitude with no adjustable parameters beyond those used to describe DIS. To calculate the forward cross section a correction for the contribution of the real part, estimated from dispersion relation arguments to be typically of order 10% [6], has to be included. Predictions for the measured total cross sections are then obtained by assuming an exponential t-distribution and integrating over t to obtain

$$\sigma_{L,T}(\gamma^* p \to \gamma p) = \frac{1}{B} \left. \frac{d\sigma^{T,L}}{dt} \right|_{t=0} \,, \tag{8}$$

where the value of the slope parameter B is taken from experiment. For this reason, the normalization is always somewhat uncertain.

In Figure 4, we compare the predictions of the FS2004 Regge and saturation models and the CGC model with the most recent data[13], using a fixed value $B = 6.02$ GeV^{-2} for the slope parameter, which was measured in the same experiment to be $6.02 \pm 0.35 \pm 0.39$. Bearing in mind the normalization uncertainty, the agreement is excellent for all three models, although significant differences between the saturated and unsaturated models appear when the predictions are extrapolated to higher energies, as one would expect.

3.2. *Diffractive deep inelastic scattering(DDIS)*

We finally turn to the so-called diffractive deep inelastic scattering (DDIS) process

$$\gamma^* + p \to X + p \;\; , \tag{9}$$

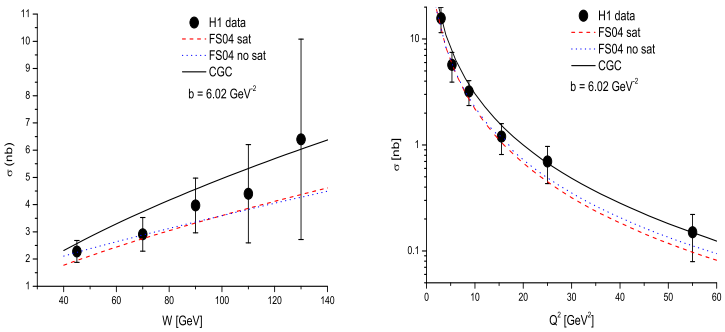

Figure 4. Comparison of the H1 DVCS data with the predictions of the FS2004 Regge model (dotted line), the FS2004 saturation model (dashed line) and the CGC saturation model (solid line). The plots show the W dependence at fixed $Q^2 = 8$ GeV^2 and the Q^2 dependence at fixed $W = 82$ GeV, respectively.

where the hadronic state X is separated from the proton by a rapidity gap. In this process, in addition to the usual variables x and Q^2 there is a third variable m_X^2, giving rise to a rich body of data. In practice, x and m_X^2 are often replaced by the variables $x_{I\!P}$ and β, given by

$$x_{I\!P} \simeq \frac{m_X^2 + Q^2}{W^2 + Q^2} \qquad \beta = \frac{x}{x_{I\!P}} \simeq \frac{Q^2}{m_X^2 + Q^2}. \tag{10}$$

in the diffractive limit $s >> Q^2, m_X^2$.

In the dipole model, the contribution due to quark-antiquark dipoles to the structure function $F_2^{D(3)}$ can be obtained from a momentum space treatment as described in [14,9]. However, if we are to confront the data at low values of β, corresponding to large invariant masses m_X, it is necessary to also include a contribution from the higher Fock state $q\bar{q}g$. We can estimate this contribution using an effective "two-gluon dipole" approximation due to Wüsthoff[14], as illustrated in Figure 5.

Again, the predictions obtained in this way involve no adjustment of the dipole cross sections and photon wavefunctions used to describe the F_2 data. However, we are again free to adjust the forward slope for inclusive diffraction, B, within the range acceptable to experiment, which means that the overall normalization, but not the energy dependence, of $F_2^{D(3)}$ is free to vary somewhat. We are also somewhat free to vary the value of α_s used to define the normalization of the model dependent $q\bar{q}g$ component, which is important at low values of β. Rather arbitrarily we take $\alpha_s = 0.1$.

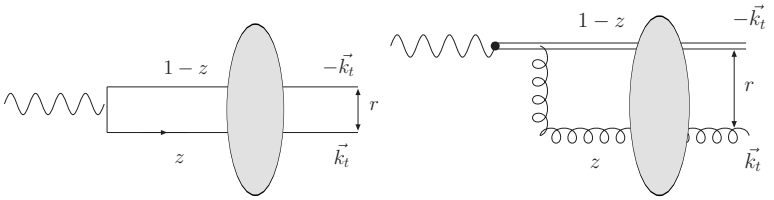

Figure 5. The $q\bar{q}$ and $q\bar{q}g$ contributions to $F_2^{D(3)}$.

In Figure 6 we compare the recent ZEUS LPS data [15] on the $x_{I\!P}$ dependence of the structure function $F_2^{D(3)}$ at various fixed Q^2 and β with the predictions obtained from the FS2004 Regge and saturation models and the CGC model. The agreement is in general good, except at the larger $x_{I\!P}$ values, corresponding to low energies, where there is clearly a significant non-diffractive contribution, neglected in the above predictions,

This problem is avoided in the LPC data [16], in which the non-diffractive contribution is explicitly removed in the data extraction. However this comes at the cost of including proton dissociation contributions, since the mass of the target fragments is only limited to below 2.3 GeV. The predictions of our three models are compared with this data in Figures 7 and 8, where the theory curves have been divided by 0.7 to allow for proton dissociation contributions, assumed to be a fixed fraction of the total, independent of the kinematic variables. This is obviously a crude approximation. Nonetheless, the agreement is remarkably good for the saturation models, except for the bins with both the lowest Q^2 values and the highest β values, corresponding to the lowest masses M_X, in the resonance region.

4. Conclusion

The colour dipole model offers a successful unified picture of diffractive photoprocesses over a wide range of Q^2, with a preference for dipole cross sections incorporating some form of saturation.

Acknowledgments

This research was supported in part by a UK Particle Physics and Astronomy Research Council grant number PPA/G/0/2002/00471.

References

1. N.N. Nikolaev and B.G. Zakharov, Z. Phys. **C49** (1991) 607; **C53** (1992) 331.

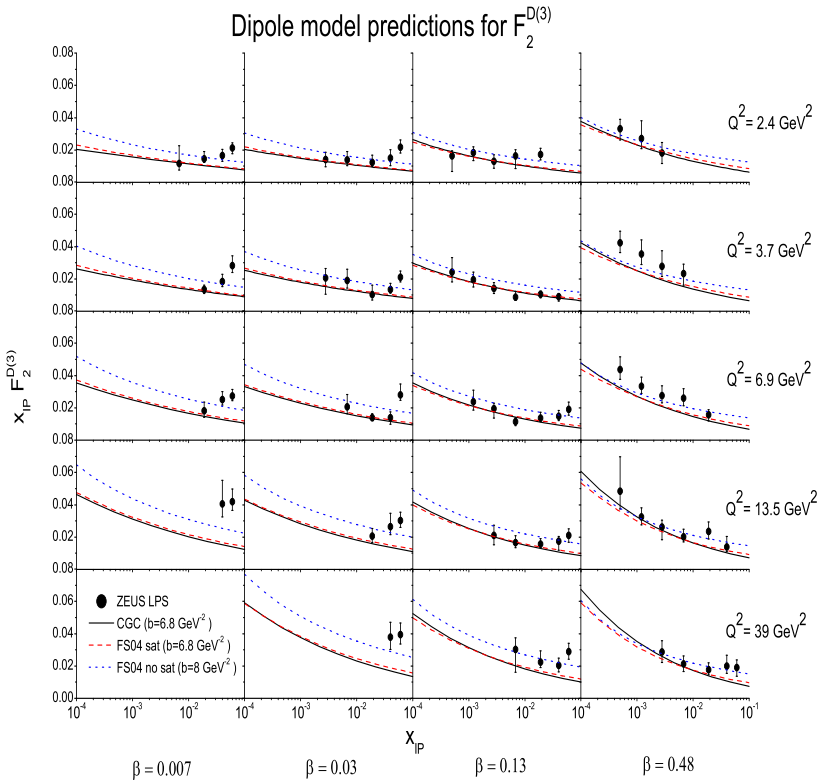

Figure 6. Predictions for the ZEUS LPS data: FS2004 Regge model (dotted line), the FS2004 saturation model (dashed line) and the CGC model (solid line)

2. A.H. Mueller, Nucl. Phys. **B415** (1994) 273; A.H. Mueller and B. Patel, Nucl. Phys. **B425** (1994) 471.
3. H.G. Dosch, T. Gousset, G. Kulzinger and H.J. Pirner, Phys. Rev. **D55** (1997) 2602.
4. J.R. Forshaw and G. Shaw, JHEP 0412 (2004) 052
5. J.R. Forshaw, G. Kerley and G. Shaw, Phys. Rev. **D60** (1999) 074012; J.R. Forshaw, G. Kerley and G. Shaw, Nucl. Phys. **A675** (2000) 80.
6. M.F. McDermott, R. Sandapen and G. Shaw, Eur. Phys. J. **C22** (2002) 665.
7. M. McDermott, L. Frankfurt, V. Guzey and M. Strikman, Eur. Phys. J. **C16** (2000) 641.

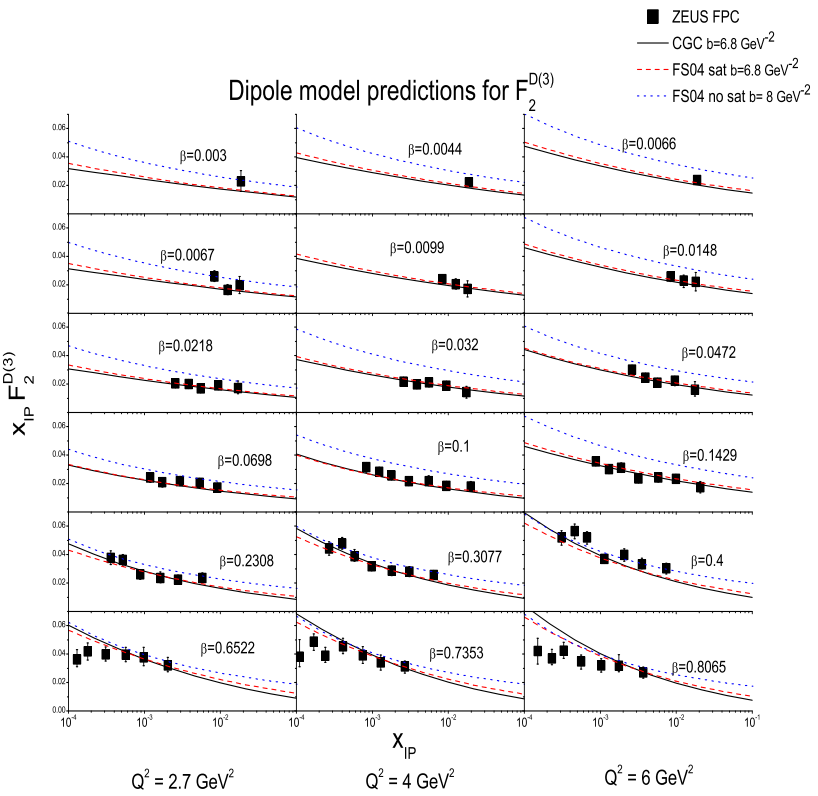

Figure 7. Predictions for the ZEUS FPC data at low Q^2: FS2004 Regge model(dotted line), the FS2004 saturation model (dashed line) and the CGC model (solid line)

8. E. Iancu, K. Itakura and S. Munier, Phys. Lett. **B590** (2004) 199.
9. K. Golec-Biernat and M. Wüsthoff, Phys. Rev. **D59** (1999) 014017; K. Golec-Biernat and M. Wüsthoff, Phys. Rev. **D60** (1999) 114023.
10. S. Chekanov et al., ZEUS Collab., Eur. Phys. J. **C21** (2001) 442.
11. C. Adloff et al., H1 Collab., Eur. Phys. J. **C21** (2001) 33.
12. H1 Collaboration: Proc. of the International Europhysics Conference on High Energy Physics, Aachen, July 2003.
13. A. Aktas et al., H1 Collab., Eur. Phys. **C44** (2005) 1.
14. M Wüsthoff, Physical Review **D56** (1997) 4311.
15. S. Chekanov et al., ZEUS Collab., Eur. Phys. J. **C38** (2004) 43.

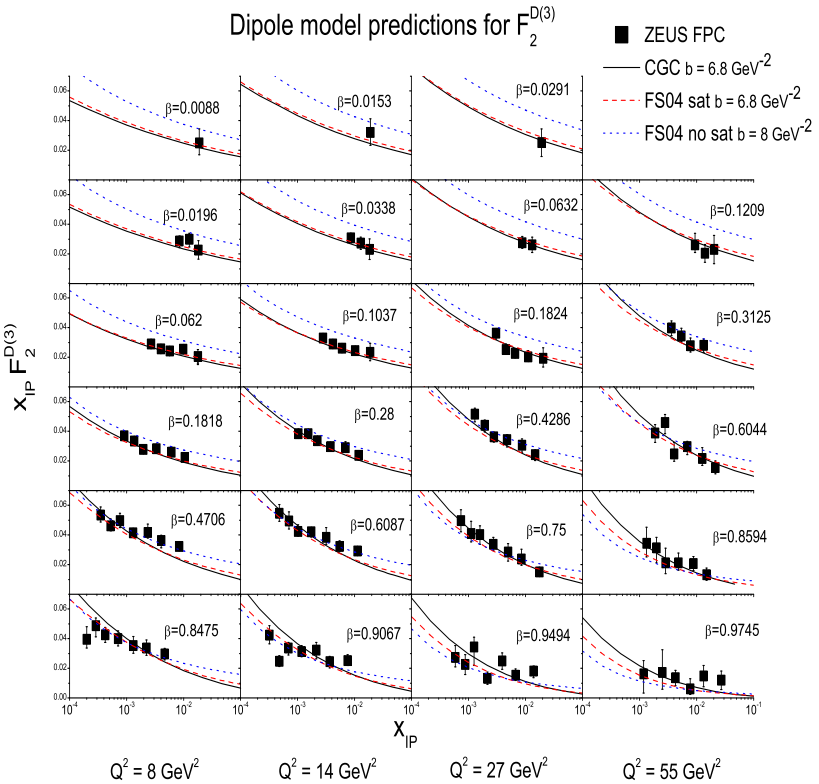

Figure 8. Predictions for the high Q^2 ZEUS FPC data: FS2004 Regge model(dotted line), the FS2004 saturation model (dashed line) and the CGC model (solid line)

16. S. Chekanov et al., ZEUS Collab., Nucl. Phys. **B713** (2005) 3.